

Gaussian effective potential: Quantum mechanics

P. M. Stevenson

Physics Department, University of Wisconsin, Madison, Wisconsin 53706

(Received 9 April 1984)

We advertise the virtues of the Gaussian effective potential (GEP) as a guide to the behavior of quantum field theories. Much superior to the usual one-loop effective potential, the GEP is a natural extension of intuitive notions familiar from quantum mechanics. A variety of quantum-mechanical examples are studied here, with an eye to field-theoretic analogies. Quantum restoration of symmetry, dynamical mass generation, and "quantum-mechanical resuscitation" are among the phenomena discussed. We suggest how the GEP could become the basis of a systematic approximation procedure. A companion paper will deal with scalar field theory.

I. INTRODUCTION

The one-loop effective potential¹ (1LEP) has become a very popular field-theoretic tool for assessing the impact of quantum effects on the classical potential. The purpose of this paper is to advertise the attractions of a similar, but superior, object, which we call the "Gaussian effective potential" (GEP). We hasten to say that the concept is not novel, having been reinvented several times.²⁻⁷ Our role is that of advocate, only. We argue that, as compared to the 1LEP, the GEP is (i) conceptually superior, (ii) more reliable, in both quantitative and qualitative terms, and (iii) almost equally easy to calculate. We support these contentions by presenting results for a variety of quantum-mechanical models, where the physics is well understood and where exact results are available for comparison.

The GEP concept²⁻⁷ is best described as a means of formalizing our intuitive understanding of zero-point fluctuation effects in quantum mechanics (QM) in a way which carries over directly to field theory. For this reason we think it is very important to have a good understanding of the QM case. In a companion paper we discuss the application to scalar field theories.⁸

Here, we study QM systems governed by a Hamiltonian

$$H = \frac{1}{2}p^2 + V(\phi), \quad (1.1)$$

with ϕ and p being conjugate operators, $[p, \phi] = -i\hbar$. This mathematical structure can be described in two different physical languages. In the usual QM language one speaks of a particle (of unit mass) in a potential $V(\phi)$, with ϕ and p being the particle's position and momentum operators, respectively. In this case, the particle moves only in one spatial dimension. For a two-dimensional system the position becomes a vector $\vec{\phi}$ with Cartesian coordinates ϕ_1, ϕ_2 and the Hamiltonian becomes

$$H = \frac{1}{2}p_1^2 + \frac{1}{2}p_2^2 + V(\phi_1, \phi_2). \quad (1.2)$$

Similarly, one can generalize to N -dimensional systems.

However, in the quantum field theory (QFT) language,⁹ the word "dimensions" takes on a different meaning. One imagines a spacetime consisting of (one point) \otimes (time).

On this "(0 + 1)-dimensional" spacetime lives a quantum field $\phi = \phi(t)$, whose dynamics is governed by the Lagrangian

$$\mathcal{L} = \int dt \left[\frac{1}{2}(\partial_t \phi)^2 - V(\phi) \right] \quad (1.3)$$

and hence by the Hamiltonian (1.1), with $p = -i\partial_t \phi$ ($\partial_t \equiv d/dt$). For example, a simple-harmonic-oscillator potential $V(\phi) = \frac{1}{2}m^2\phi^2$ corresponds to a (0 + 1)-dimensional free field theory. The system (1.2) is also to be thought of as a (0 + 1)-dimensional field theory, but now there are two fields, ϕ_1 and ϕ_2 , which are coupled in a certain way. We shall make use of both languages: indeed, our aim is essentially to transcribe the intuition familiar in QM terms into the QFT language.

We begin by motivating and defining the Gaussian effective potential in Sec. II. Our discussion here is very qualitative and informal. In Sec. III we present quantitative results for a variety of interesting potentials. Section IV describes the GEP formalism for two-dimensional systems (two coupled fields), and applies it to the O(2)-symmetric anharmonic oscillator (Goldstone potential), and to a coupled oscillator model exhibiting dynamical mass generation. Section V deals with the relationship with the Caswell-Killingbeck (CK) method,¹⁰⁻¹² which suggests a means by which the GEP could be made the basis for a systematic approximation scheme for field theory.

II. THE MOTIVATION FOR THE GEP

In QM one has quite a good intuitive understanding of the effects of quantum fluctuations. This intuition is partially summarized by the statement that a *quantum-mechanical particle does not like to live in a narrow potential well*. This "quantum claustrophobia" arises from the uncertainty principle: If the particle's wave function is concentrated in a small spatial region $\Delta\phi$, then the momentum uncertainty is correspondingly large ($\Delta p \geq \hbar/\Delta\phi$), and so there is a large contribution to the energy arising from the kinetic term $\langle \frac{1}{2}p^2 \rangle$. Hence, the ground-state (GS) energy is influenced not just by the *depth*, but also by the *width* of the potential well(s). A

familiar example is the zero-point energy $\frac{1}{2}\hbar\omega$ of the harmonic-oscillator potential, $V(\phi) = \frac{1}{2}\omega^2\phi^2$. In this way a quantum particle tends to resist being confined in a small space.

Without this effect, the world as we know it would collapse. The Coulomb potential $-e^2/r$ in an atom is unbounded below, so classically the electron should simply fall into the nucleus. It is the quantum fluctuation effects which prevent this disaster. The quantum claustrophobia of the electron enables it to resist the seemingly irresistible attraction of the classical potential, and the net result is a compromise; a finite-energy ground state, centered on the origin, but with a definite spatial extent. (The phenomenon has been aptly named¹³ "quantum-mechanical resuscitation," since a system which is sick, classically, is restored to life by QM fluctuation effects.) It is natural to describe the situation in terms of an "effective" potential, which, in some vague sense, gives a picture of how the quantum fluctuations modify the classical potential. For the hydrogen atom problem it would look something like Fig. 1.

Some other examples of how quantum effects may qualitatively change a system's behavior are illustrated in Fig. 2 in terms of an "effective" potential. Consider a symmetric double-well potential. To begin with, suppose the quantum effects are relatively small [Fig. 2(a)]. The effective potential is then little different from the original potential; slightly higher in the wells, due to the $\frac{1}{2}\hbar\omega_{\text{eff}}$ zero-point energy, and slightly lower in the barrier region, since by "spreading itself out" the particle is able to lower its energy. If, however, the quantum effects are large, then the particle does not see two separate wells but perceives only the outer walls as forming one large well—with the "barrier" being no more than an irrelevant bump at the bottom. The effective potential is a simple U shape, centered on the origin. [See Fig. 2(b).] In QFT language this would be described as "symmetry restoration by quantum effects."¹⁴ We shall see this effect quantitatively in Sec. III A.

Our other example is a particular type of asymmetric double-well potential, consisting of a broad well and a

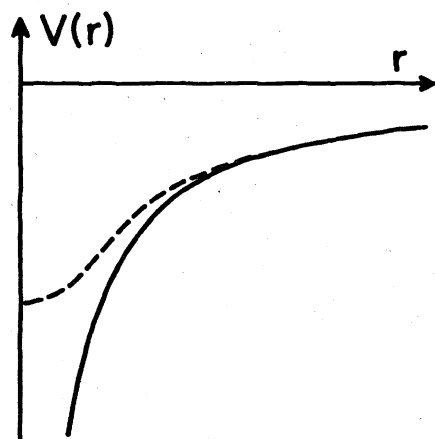


FIG. 1. The Coulomb potential. The effect of quantum fluctuations is pictured in terms of an "effective" potential (dashed curve).

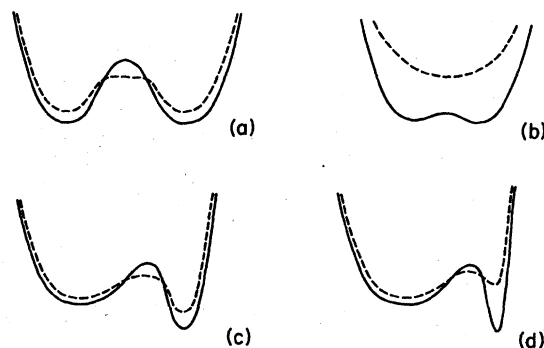


FIG. 2. "Effective" potentials for some double-well examples. In (a) and (c) the parameters are such that the quantum effects are relatively small. In (b) and (d) the quantum effects are large and qualitatively alter the physics. (As with Figs. 1 and 3, these are sketches only: quantitative examples are discussed in Secs. III and IV.)

slightly deeper, but much narrower, well. If the quantum effects are relatively small, then the effective potential is qualitatively similar to the classical potential [Fig. 2(c)], and the ground state remains in the deeper, narrower well. Now we adjust the potential's parameters such that the narrow well is made narrower and narrower. Eventually, the zero-point energy will become so large that the particle will prefer to reside in the broader well, even though it has a higher classical energy [Fig. 2(d)]. In QFT terms, the "false vacuum" of the classical theory has become the "true vacuum" of the quantum theory, and vice versa. In Sec. III B we shall see an example which "almost" shows this effect.

So far we have been deliberately vague as to what exactly we mean by the effective potential. Our examples above were intended to convey some feeling for how an effective potential should look, if it is to serve as a pictorial representation of our intuitive understanding. We now consider how to define an object which embodies these ideas.

First, the effective potential we have been discussing is certainly not what is usually called "the effective potential."¹⁵ (A nice discussion of the effective potential in QM has been given by Curtright and Thorn,¹⁶ and our remarks here are mostly borrowed from them.) The conventional effective potential is defined by

$$V_{\text{eff}}(\phi_0) = \min_{\{\psi\}} \langle \psi | H | \psi \rangle, \quad (2.1)$$

with ψ subject to

$$\langle \psi | \psi \rangle = 1, \quad \langle \psi | \phi | \psi \rangle = \phi_0. \quad (2.2)$$

This means that one should consider the expectation value of the energy obtained with all possible normalized wave functions centered on ϕ_0 (in the sense that the expectation value of ϕ is ϕ_0). The effective potential at ϕ_0 is the minimum such energy expectation value. Notice that, even in QM, the procedure involves a functional minimization (normally handled by a Lagrange-multiplier technique^{15,16}). The most important property of $V_{\text{eff}}(\phi_0)$ is that its global minimum gives the exact GS energy of the system.

Another important feature is that $V_{\text{eff}}(\phi_0)$ is convex (i.e., $d^2 V_{\text{eff}}/d\phi_0^2 \geq 0$).^{17,16} This is most undesirable from our point of view. It means that $V_{\text{eff}}(\phi_0)$ can never have a double-well shape, even in cases [e.g., Fig. 2(a)] where this is the natural way to describe the physics. Instead, one gets the kind of absurdity seen in Fig. 3(a), where $V_{\text{eff}}(\phi_0)$ has its minimum value right in the middle of a very real potential barrier. Some recent papers have helped to elucidate this curious phenomenon.^{18,16} The essential point is that the condition $\langle \psi | \phi | \psi \rangle = \phi_0$ only requires the wave function to be “centered” on ϕ_0 in a purely nominal sense. It could, for instance, consist of two large peaks on either side of ϕ_0 , with $|\psi|^2$ being small in the neighborhood of ϕ_0 . As an analogy, consider a commuter who works in the inner city but who lives in the countryside. His mean position is somewhere in the inner suburbs, but he sees that locality only for a few seconds per day as he flashes past in the train. His experience of life tells us nothing about life in the inner suburbs. In the same way, the effective potential at a point ϕ_0 may not give a good indication of conditions there. Instead, it may be giving some average of conditions in two or more regions either side of ϕ_0 . It is due to this effect that the effective potential misleadingly wipes out very real barriers, as in Fig. 3(a).

Another bizarre consequence is seen in Fig. 3(b). For any potential which tends to a finite value at infinity, as in many QM problems, $V_{\text{eff}}(\phi_0)$ equals E_0 for *all* ϕ_0 .¹⁶ This gives a misleading impression that the particle is free to wander anywhere, whereas of course it remains localized in the potential well. The moral of these examples is that $V_{\text{eff}}(\phi_0)$ does not in general give a good “picture” of the physics,¹⁶ and it cannot be the effective potential we had in mind earlier.

Nor is the one-loop effective potential adequate for our purposes. This is a semiclassical construct, based on adding to the classical potential the order- \hbar quantum corrections, and neglecting the terms of order \hbar^2 or higher. That is, if $V_{\text{eff}}(\phi_0)$ has the formal series expansion (around the hypothetical $\hbar \rightarrow 0$ limit)

$$V_{\text{eff}}(\phi_0) \sim V(\phi_0) + \sum_{n=1}^{\infty} \hbar^n V_n(\phi_0), \quad (2.3)$$

then

$$V_{1l}(\phi_0) \equiv V(\phi_0) + \hbar V_1(\phi_0). \quad (2.4)$$

The problem—quite apart from the question of whether

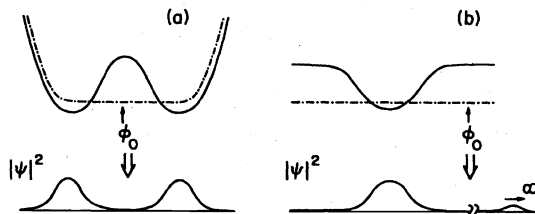


FIG. 3. Odd behavior of the conventional (so-called) effective potential for (a) the double-well potential and (b) a finite-depth potential well. Below each figure is a sketch of the wave function associated with the point ϕ_0 indicated.

the effective potential is itself a desirable goal—is that a one-loop approximation generally breaks down whenever the quantum effects become large—and, as we saw above, most of the interesting cases occur precisely when this is the case. We shall be illustrating the failings of the 1LEP later on in Secs. III and IV.

Returning to our discussion of the (exact) effective potential, we saw above that its undesirable features arose from the possibility that the trial wave functions could be double humped (or even multiple humped) and not located at ϕ_0 , except in a nominal sense. This suggests that we can obtain a more realistic effective potential by insisting that the trial wave function be genuinely concentrated in the vicinity of ϕ_0 . An obvious and attractive way of doing this is to restrict the admissible wave functions to those of Gaussian form, centered on ϕ_0 . The Gaussian function is a natural choice, being the GS wave function of the archetypal parabolic potential well. This motivates the definition of $\bar{V}_G(\phi_0)$, the Gaussian effective potential (GEP), as

$$\bar{V}_G(\phi_0) \equiv \min_{\Omega} V_G(\phi_0, \Omega) \equiv \min_{\Omega} \langle \psi | H | \psi \rangle, \quad (2.5)$$

with

$$|\psi\rangle = \left[\frac{\Omega}{\hbar\pi} \right]^{1/4} \exp \left[-\frac{1}{2} \frac{\Omega}{\hbar} (\phi - \phi_0)^2 \right], \quad \Omega > 0. \quad (2.6)$$

Note that the width of the Gaussian, governed by the parameter Ω , is left to adjust itself so as to minimize $\langle H \rangle$ at each ϕ_0 . Thus \bar{V}_G can be described as a variational approximation to V_{eff} .

As we say, this is a very natural and obvious idea, so it is not surprising that it has been invented, and reinvented, before. See Ref. 7 and Refs. 2–6. Our aim here and in Ref. 8 is to distill the essence of these ideas and present them in the simplest possible form.

The thrust of our above discussion is that \bar{V}_G should not be regarded *merely* as an approximation to V_{eff} , but as an interesting object in its own right. With its convex property, V_{eff} is not a very useful object, and does not provide a good picture of the basic physics. We can expect \bar{V}_G to be more realistic in this respect, since it expresses what it feels like to be a quantum particle “at” ϕ_0 —with the word “at” having something more like its everyday meaning than the treacherous expectation value requirement employed by V_{eff} .

We shall no longer have the property that the global minimum of \bar{V}_G gives the GS energy, as was the case with V_{eff} . However, by the Rayleigh-Ritz theorem, $\bar{V}_G(\phi_0) \geq V_{\text{eff}}(\phi_0)$ at any ϕ_0 . In most circumstances one can expect a good approximation to E_0 , for the usual variational reason that any halfway-realistic wave function generally gives a reasonable estimate of the GS energy.

A major practical advantage of \bar{V}_G is that it is *calculable*. Moreover, the calculation is rather easy, and generalizes immediately to field theory.^{2–8} The direct approach is to use the Schrödinger representation $p = -i\hbar d/d\phi$ and evaluate $\langle \psi | H | \psi \rangle$ as the integral

$$\langle H \rangle = \int_{-\infty}^{\infty} d\phi \psi^*(\phi) \left[-\frac{\hbar^2}{2} \frac{d^2}{d\phi^2} + V(\phi) \right] \psi(\phi), \quad (2.7)$$

with $\psi(\phi)$ being the Gaussian function displayed in Eq. (2.6). However, for a polynomial $V(\phi)$, one can make the calculation purely algebraic by employing the creation-annihilation operator formalism. To do this one makes the substitutions

$$\begin{aligned} \phi &= \phi_0 + \hbar(2\hbar\Omega)^{-1/2}(a_\Omega + a_\Omega^\dagger), \\ p &= -\frac{1}{2}i(2\hbar\Omega)^{1/2}(a_\Omega - a_\Omega^\dagger), \end{aligned} \quad (2.8)$$

where

$$[a_\Omega, a_\Omega^\dagger] = 1 \quad (2.9)$$

and evaluates the expectation value of H in the state $|0\rangle_\Omega$, defined by

$$a_\Omega |0\rangle_\Omega = 0. \quad (2.10)$$

The subscript Ω is a reminder that a_Ω and a_Ω^\dagger depend on the frequency of the harmonic oscillator whose ground state $|0\rangle_\Omega$ is our Gaussian trial wave function. The field-theoretic generalization is obviously to write the field $\phi(x)$ as a classical field $\phi_0(x)$ plus the usual expression for a free quantum field of mass Ω .²⁻⁸

To illustrate the procedure we consider the anharmonic-oscillator (AHO) Hamiltonian^{2,4}

$$H = \frac{1}{2}p^2 + \frac{1}{2}m^2\phi^2 + \lambda\phi^4. \quad (2.11)$$

The matrix elements of p^2 , ϕ^2 , and ϕ^4 are easily evaluated from (2.8)–(2.10), leading to

$$\begin{aligned} V_G(\phi_0, \Omega) &\equiv \langle 0 | H | 0 \rangle_\Omega \\ &= \frac{1}{4}\hbar\Omega + \frac{1}{2}m^2[\phi_0^2 + \hbar(2\Omega)^{-1}] \\ &\quad + \lambda[\phi_0^4 + 6\phi_0^2\hbar(2\Omega)^{-1} + 3\hbar^2(2\Omega)^{-2}]. \end{aligned} \quad (2.12)$$

$\bar{V}_G(\phi_0)$ itself is obtained by minimizing $V_G(\phi_0, \Omega)$ with respect to Ω . Note that Ω is positive definite, since the Gaussian wave function must be normalizable. Moreover, since the kinetic term gives rise to an Ω term, and the potential terms to inverse powers of Ω , it is clear that a minimum always exists in the range $0 < \Omega < \infty$. The equation for the optimum Ω , denoted $\bar{\Omega}$, is obtained by differentiating (2.12), and can be expressed as

$$\bar{\Omega}^3 - (m^2 + 12\lambda\phi_0^2)\bar{\Omega} - 6\hbar\lambda = 0. \quad (2.13)$$

We shall refer to this as the “optimization condition,” though it is often called the “gap equation.”¹⁹ We can use it to simplify the expression for \bar{V}_G to

$$\bar{V}_G(\phi_0) = (\frac{1}{2}m^2\phi_0^2 + \lambda\phi_0^4) + \frac{1}{2}\hbar\bar{\Omega} - \frac{3}{4}\hbar^2\frac{\lambda}{\bar{\Omega}^2}. \quad (2.14)$$

We shall often drop the overbar on Ω where no confusion can arise.

There is a close connection here with the method of Caswell¹⁰ and Killingbeck¹¹ for obtaining eigenvalues of the AHO with a modified form of perturbation theory in which

$$\begin{aligned} H_0 &= \frac{1}{2}(p^2 + \Omega^2\phi^2), \\ H_{\text{int}} &= \lambda\phi^4 + \frac{1}{2}(m^2 - \Omega^2)\phi^2. \end{aligned} \quad (2.15)$$

(See also Ref. 12.) The arbitrary frequency parameter Ω is chosen such that each approximate eigenvalue is stationary with respect to variations in Ω about $\bar{\Omega}$.^{10,11} (This requires a different $\bar{\Omega}$ for each eigenvalue, and for each eigenvalue $\bar{\Omega}$ changes from order to order.) Although for the excited states one no longer has a Rayleigh-Ritz inequality to rigorously justify this choice of Ω , one can still argue strongly that this is a sensible procedure.^{10,11,20} The point is that the exact eigenvalues are obviously Ω independent, and so the results of the procedure implied by (2.15) are only believable when they are at least approximately Ω independent.

It should be obvious that the first-order result of this procedure applied to the ground state yields precisely the $\phi_0=0$ value of \bar{V}_G . Thus, the GEP can be viewed as a generalization of the Caswell-Killingbeck (CK) procedure, incorporating a translation of the field (position operator) ϕ . This additional feature gives us a great advantage over the CK procedure in the case of the double-well potential ($m^2 < 0$), where the minimum energy state is not necessarily located at the origin.

However, in many ways it is the CK procedure which is the more general, since it applies to any eigenvalue, not just the lowest. (It can also be made into a method for computing accurate wave functions.²¹) Most importantly, it supplies a systematic procedure for steadily improving the results. Our hope is that by combining the GEP concept²⁻⁶ with the CK procedure¹⁰⁻¹² one can build a much superior alternative to the conventional loop expansion/perturbation theory methods in field theory.

We postpone further discussion of these matters until Sec. V, but we do note here that one can immediately define an excited-state generalization of \bar{V}_G by

$$\bar{V}_{G,j}(\phi_0) \equiv \min_{\Omega} V_{G,j}(\phi_0, \Omega) \equiv \min_{\Omega} \langle j | H | j \rangle_{\Omega}, \quad (2.16)$$

where

$$|j\rangle_{\Omega} \equiv (j!)^{-1/2}(a_{\Omega}^{\dagger})^j |0\rangle_{\Omega}. \quad (2.17)$$

In other words, our trial wave function is now the j th excited state, rather than the ground state, of a harmonic oscillator of frequency Ω , i.e., a Gaussian times the j th Hermite polynomial. Estimates for the excited-state eigenvalues can be obtained from the minima of the $\bar{V}_{G,j}(\phi_0)$ potentials, and we shall investigate this a little in Sec. III. Note that the ϕ_0 identified as the location of the ground state is not necessarily relevant for calculating the excited-state eigenvalues. For example, in an asymmetric potential well the centroid of the first excited-state wave function is shifted relative to the GS wave function.

Finally, we describe the connection between the GEP and the 1LEP. We have laboriously kept all the \hbar factors to facilitate this. (In later sections we set $\hbar=1$.) The GEP calculation actually contains within it the one-loop result.⁴ All one need do is to drop the \hbar^2 term in (2.12) and, in consequence, the \hbar term in (2.13). The optimization condition then reduces to

$$\bar{\Omega}^2 = m^2 + 12\lambda\phi_0^2 = V''(\phi_0), \quad (2.18)$$

where the relation to the second derivative of the classical potential is true quite generally. Using (2.14), again discarding the \hbar^2 term, we have

$$V_{1l}(\phi_0) = V(\phi_0) + \frac{1}{2}\hbar[V''(\phi_0)]^{1/2}. \quad (2.19)$$

(The positive square root is required, since $\Omega > 0$.)

It is amusing to check that this is indeed the 1LEP, as understood by field theorists, by performing the diagram summation in the manner of Coleman and Weinberg¹ in $0+1$ dimensions. [For the $(0+1)$ -dimensional Feynman rules see Ref. 9.] This gives the one-loop correction term in the form

$$\begin{aligned} \hbar \sum_{n=1}^{\infty} \frac{1}{2n} \int_{-\infty}^{\infty} \frac{dk}{2\pi} \left[\frac{4! \lambda \frac{1}{2} \phi_0^2}{k^2 + m^2} \right]^n \\ = \frac{1}{2}\hbar \int_{-\infty}^{\infty} \frac{dk}{2\pi} \ln \left[1 + \frac{12\lambda\phi_0^2}{k^2 + m^2} \right] \\ = \frac{1}{2}\hbar[(m^2 + 12\lambda\phi_0^2)^{1/2} - m]. \end{aligned} \quad (2.20)$$

[The extra $-\frac{1}{2}\hbar m$ term is simply a reflection of the fact that the Coleman-Weinberg calculation implicitly involves a redefinition of the zero of the energy scale so that $V_{1l}(\phi_0=0)=0$.]

Note that, whereas $\bar{V}_G(\phi_0)$ is always well defined and real, $V_{1l}(\phi_0)$ becomes ill defined and complex whenever $V''(\phi_0)$ is negative. It is important to realize that this is purely an artificial pathology of the 1LEP, not a pathology of the physics. This, and other matters, will perhaps be clarified by the quantitative examples we show in the next two sections.

III. QUANTITATIVE EXAMPLES

A. The anharmonic-oscillator/double-well potential

We now turn to a quantitative discussion of the GEP applied to the familiar potential

$$V(\phi) = \sigma + \frac{1}{2}m^2\phi^2 + \lambda\phi^4, \quad (3.1)$$

which is the anharmonic oscillator (AHO) for $m^2 > 0$, and the standard double-well potential (DWP) for $m^2 < 0$. We choose the constant term such that the classical GS energy is zero, i.e.,

$$\sigma \equiv \begin{cases} 0, & m^2 > 0 \\ m^4/(16\lambda), & m^2 < 0. \end{cases} \quad (3.2)$$

From now on we set $\hbar=1$. Following the usual practice we quote energies in units of $|m|$ in Table I. However, in some ways it is more helpful to imagine λ as fixed, with m^2 as the adjustable parameter. For this reason we introduce a "dimensionless mass" parameter

$$\xi^2 \equiv m^2/(2\lambda)^{2/3}. \quad (3.3)$$

Then we have the following correspondences:

$$\begin{aligned} \xi^2 \rightarrow +\infty & \text{ weak coupling,} \\ \xi^2 = 0 & \text{ strong coupling (quartic oscillator),} \\ \xi^2 \rightarrow -\infty & \text{ two independent harmonic wells.} \end{aligned}$$

Table I shows the GEP results for the GS energy over the whole range of ξ^2 . The entries have been selected for ease of comparison with readily accessible "exact" numerical results. For the AHO we have utilized Table II of Ref. 10, and for the DWP we have used Table IV of Ref. 22.

TABLE I. Approximate GS energies for the AHO/DWP obtained from the GEP. See Eqs. (3.4) and (3.5) for $\xi^2 > -3.385$ and (3.8) and (3.9) for $\xi^2 < -3.385$. Energies are quoted relative to the classical ground state as zero, so the error column represents the percentage by which the GEP result overestimates the quantum zero-point energy.

ξ^2	$\lambda/ m ^3$	$\bar{\Omega}/ m $	$E_0^{(G)}/ m $	Error (%)
$+\infty$	0	1	$\frac{1}{2}$	0
13.572...	0.01	1.028 75	0.507 288	0.006
2.924...	0.1	1.221 20	0.560 307	0.21
0.630...	1.0	2.000 00	0.812 500	1.09
0.136...	10.0	4.000 00	1.531 250	1.75
0.029...	100.0	8.473 85	3.192 444	1.95
0	∞	$(6\lambda)^{1/3}$	$(0.6814)\lambda^{1/3}$	2.01
-0.5	1.414...	1.876 60	0.681 309	3.32
-1	0.5	1.213 41	0.477 014	5.11
-2	0.177...	0.707 11	0.441 942	9.86
-4	0.0625...	1.164 44	0.651 360	11.84
-5	0.045...	1.253 78	0.669 565	5.44
-7	0.027...	1.324 95	0.685 542	1.36
-10	0.016...	1.364 15	0.694 821	0.64
-50	0.001...	1.409 95	0.706 043	0.05
$-\infty$	0	$\sqrt{2}$	$\sqrt{2}/2$	0

(Note that their Z^2 corresponds to our $-\xi^2$.)

The formulas for constructing $\bar{V}_G(\phi_0)$ have already been given in Eqs. (2.13) and (2.14). For the AHO, $\infty > \xi^2 > 0$, the shape of $\bar{V}_G(\phi_0)$ can easily be imagined, and so we do not show a figure. The minimum is of course at the origin, and it yields the following estimate of the ground-state energy E_0 :

$$\bar{V}_G(\phi_0=0) = \frac{1}{2}\Omega \left[1 - \frac{3}{2} \frac{\lambda}{\Omega^3} \right] + \sigma, \quad (3.4)$$

where

$$\Omega^3 - m^2\Omega - 6\lambda = 0. \quad (3.5)$$

As noted earlier, this is exactly the same as applying the first-order CK method. The result is accurate to within 2% even in the strong-coupling limit,^{4,10} as seen in the first part of Table I. By contrast, the one-loop approach gives an estimate of E_0 which is $\frac{1}{2}m$ for all λ . This is accurate for weak coupling, but it becomes quite unrealistic for $\lambda \gtrsim 1$. The problem is simply that V'' at the origin is then not a good measure of the effective width of the well.

In the DWP case the situation is more interesting. With ξ^2 negative, but small, the GEP retains a single-well shape, showing the "symmetry restoration" phenomenon described earlier. As ξ^2 becomes still more negative, $\bar{V}_G(\phi_0)$ evolves into a double-well form. The two cases are exemplified by $\xi^2 = -1$ [Fig. 4(a)] and $\xi^2 = -10$ [Fig. 4(b)]. One can easily show that in all cases the origin is a *minimum*, never a maximum, since

$$d^2\bar{V}_G/d\phi_0^2|_{\phi_0=0} = \Omega^2|_{\phi_0=0} > 0. \quad (3.6)$$

For small negative ξ^2 this minimum continues to provide us with our estimate of the ground-state energy. However, for $\xi^2 < -3.385044$ there is a deeper minimum at the position

$$\phi_{0,\min} = \left[-\frac{1}{4\lambda} \left[m^2 + \frac{6\lambda}{\Omega} \right] \right]^{1/2}, \quad (3.7)$$

with energy

$$\bar{V}_G(\phi_{0,\min}) = \frac{1}{2}\Omega(1 + 3\lambda/\Omega^3), \quad (3.8)$$

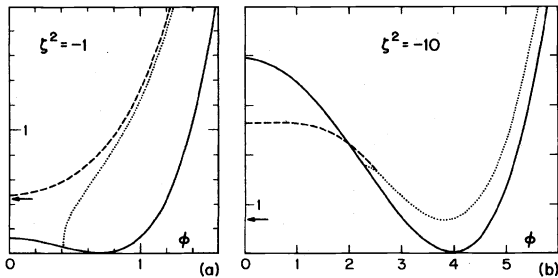


FIG. 4. Effective potentials for the double-well potential; (a) $\xi^2 = -1$ ($\lambda/|m|^3 = 0.5$) and (b) $\xi^2 = -10$ ($\lambda/|m|^3 = 0.015811$). Solid curve = potential; dashed curve = GEP; dotted curve = 1LEP. The arrow indicates the exact GS energy. Only the right-hand half of the symmetric potential is shown. The GEP and 1LEP almost coincide for large ϕ_0 .

where Ω is the larger positive root of

$$\Omega^3 + 2m^2\Omega + 12\lambda = 0. \quad (3.9)$$

[The other positive root corresponds to the local maximum of $\bar{V}_G(\phi_0)$ between $\phi_{0,\min}$ and the origin.] Thus for large negative ξ^2 , our estimate of the GS energy comes from Eqs. (3.8) and (3.9). As $\xi^2 \rightarrow -\infty$ this estimate becomes exact because the system becomes essentially two independent harmonic-oscillator wells. This provides a substantial improvement over the CK method, which remains committed to the $\phi_0=0$ result and which becomes progressively worse as $\xi^2 \rightarrow -\infty$.

As shown in Table I, the GEP gives a good estimate of E_0 for all values of ξ^2 . The worst case occurs for $\xi^2 \simeq -3$, in the transition region between single-well and double-well behavior. Nevertheless, the GEP results remain reasonably satisfactory even here. Extrapolating from the tabulated values, we estimate that the error is never worse than about 20%.

In contrast, the 1LEP shows pathological behavior. It is very similar to the GEP at large ϕ_0 , but quits abruptly when the second derivative of the classical potential becomes negative. (See the dotted lines in Fig. 4.) For small ϕ_0 the 1LEP is undefined—or, if preferred, it may be said to have an imaginary part. According to folklore, this is supposed to be an indication of some sort of instability at small ϕ_0 . Clearly, this is not the case for small negative ξ^2 , as in Fig. 4(a), where the GS wave function is actually concentrated at small ϕ_0 .

Returning to the GEP, we can extend the results to the excited states by computing the excited-state generalization of \bar{V}_G defined in Eqs. (2.16) and (2.17). The calculation is almost equally simple and gives

$$\bar{V}_{G,j}(\phi_0) = V(\phi_0) + (j + \frac{1}{2})\Omega - \frac{3}{4}(2j^2 + 2j + 1)\lambda/\Omega^2, \quad (3.10)$$

where

$$\Omega^3 - (m^2 + 12\lambda\phi_0^2)\Omega - 6\lambda(2j^2 + 2j + 1)/(2j + 1) = 0. \quad (3.11)$$

When this potential has its global minimum at $\phi_0=0$, as is always the case for the AHO ($\xi^2 > 0$), our eigenvalue estimates coincide with the first-order CK method. This is known to give excellent results, even in the strong-coupling limit.^{4,10,11} (For $\xi^2=0$, the errors interpolate smoothly between +2% for $j=0$ to -1% for $j \rightarrow \infty$.) For the DWP at large negative ξ^2 , $\bar{V}_{G,j}(\phi_0)$ has basically a double-well shape for small j , evolving to a single-well shape for large j . This corresponds to the low-lying states being located within one or other of the two wells, while the high-lying states above the barrier see only a single overall well. Note that j does not necessarily correspond to the principal quantum number, as the states may have to be renumbered: When $\bar{V}_{G,j}(\phi_0)$ has its minimum away from the origin, it indicates a *pair* of degenerate states, one in each well. In reality, of course, these "degenerate" states are split by a small amount, due to tunneling between the two wells, but the GEP is blind to this small effect. [However, when tunneling becomes a large effect, it

is seen by the GEP through the lowering of the effective barrier (cf. Fig. 4).]

As far as we can tell from the rather limited comparison with the exact results of Ref. 22, we obtain a reasonable description of the DWP eigenvalues by this means. It is rather remarkable that in just two simple equations, (3.10) and (3.11), one can summarize an approximate description of the entire energy-level structure of the AHO/DWP for all coupling strengths.

B. An asymmetric double-well potential

It is quite straightforward to extend the calculations to a general sextic potential

$$V(\phi) = \sum_{n=0}^6 c_n \phi^n. \quad (3.12)$$

$$\bar{V}_{G,j} = V(\phi_0) + J\Omega - \frac{3(4J^2+1)}{8\Omega^2}(c_4 + 5c_5\phi_0 + 15c_6\phi_0^2) - \frac{5J(4J^2+5)}{4\Omega^3}c_6, \quad (3.14)$$

with Ω given by

$$-4J\Omega^4 + 8J(c_2 + 3c_3\phi_0 + 6c_4\phi_0^2 + 10c_5\phi_0^3 + 15c_6\phi_0^4)\Omega^2 + 6(4J^2+1)(c_4 + 5c_5\phi_0 + 15c_6\phi_0^2)\Omega + 15J(4J^2+5)c_6 = 0. \quad (3.15)$$

The particular example we wish to discuss is a potential of the form

$$V(\phi) = \frac{1}{2}[v^2(\phi) + v'(\phi)], \quad (3.16)$$

with

$$v(\phi) = (1 + \phi^2)(1 - m\phi), \quad (3.17)$$

which arises in a supersymmetric QM model studied by Karsch, Rabinovici, Shore, and Veneziano (KRSV).²³ We shall not discuss the supersymmetry aspects here: for our purposes the potential is simply an interesting example for which some exact results are known. The special features of this kind of potential are (i) the GS energy is exactly zero, with the GS wave function being $\exp[\int v(\phi)d\phi]$, and (ii) for small m it is "almost" an example of quantum effects interchanging the roles of true and false vacua, as discussed in Sec. II [see Fig. 2(d)]. We say almost because here the ground state remains localized in the deeper, narrower well, as in the classical case, but all the other low-lying states are associated with the higher but broader well (for sufficiently small m).²³

We see this phenomenon very nicely through the GEP. Figure 5 shows the case $m=0.2$. The ground state corresponds to the minimum of the GEP (dashed line), which occurs in the right-hand well and has a value of approximately zero. The GEP has another prominent minimum in the left-hand well. This corresponds to the first excited state of the system, having much lower energy than a one-quantum excitation in the very narrow well, as can be seen by comparison with $\bar{V}_{G,1}(\phi_0)$ (dot-dashed curve). The second excited state of the system is a one-quantum excitation in the broader well, corresponding to the lowest minimum of $\bar{V}_{G,1}(\phi_0)$. (For the higher states the situation is complicated, since we enter the transition region to

The required matrix elements, in terms of $J \equiv j + \frac{1}{2}$, are

$$\begin{aligned} \langle j | p^2 | j \rangle &= J\Omega, \\ \langle j | \phi | j \rangle &= \phi_0, \\ \langle j | \phi^2 | j \rangle &= \phi_0^2 + J/\Omega, \\ \langle j | \phi^3 | j \rangle &= \phi_0^3 + 3J\phi_0/\Omega, \\ \langle j | \phi^4 | j \rangle &= \phi_0^4 + 6J\phi_0^2/\Omega + 3(4J^2+1)/(8\Omega^2), \\ \langle j | \phi^5 | j \rangle &= \phi_0^5 + 10J\phi_0^3/\Omega + 15(4J^2+1)\phi_0/(8\Omega^2), \\ \langle j | \phi^6 | j \rangle &= \phi_0^6 + 15J\phi_0^4/\Omega + 45(4J^2+1)\phi_0^2/(8\Omega^2) \\ &\quad + 5J(4J^2+5)/(8\Omega^3). \end{aligned} \quad (3.13)$$

From these results we find the generalized GEP can be written as

single-well behavior.) This picture of the energy-level structure, and the kind of wave functions it implies, compares very well with the numerically computed results of KRSV in their Figs. 3, 4, and 6. A comparison of the approximate eigenvalues from the GEP with the exact results is shown in Table II.

With the GEP it is easy to proceed to smaller values of m (whereas numerical integration of the Schrödinger

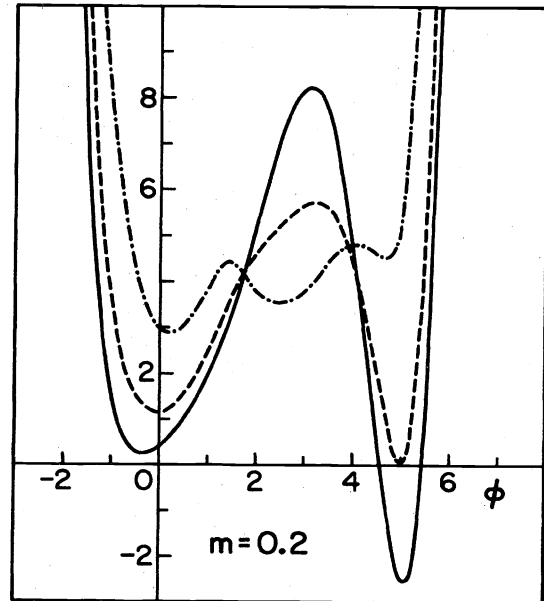


FIG. 5. The KRSV potential, Eqs. (3.16) and (3.17) with $m=0.2$. The GEP is the dashed curve, and its first-excited-state generalization is the dot-dashed curve. (See Figs. 3, 4, and 6 of Ref. 23.)

TABLE II. Eigenvalues for the KRSV potential, Eqs. (3.16) and (3.17) showing the comparison between the approximate values obtained from the GEP and the exact values from Ref. 23.

	GEP	Exact
$E_0(m=0.2)$	0.036	0
$E_1(m=0.2)$	1.17	1.15
$E_2(m=0.2)$	2.88	2.91
$E_0(m=0.5)$	0.13	0
$E_1(m=0.5)$	1.03	1.02
$E_2(m=0.5)$	2.30	2.40

equation becomes progressively harder). One sees clearly the phenomenon described by KRSV, with the spectrum tending to that of $V(\phi) = \frac{1}{2}[(1+\phi^2)^2 + 2\phi]$ [the $m \rightarrow 0$ limit of Eqs. (3.16) and (3.17)], but with an extra state—the ground state, with $E_0=0$ and $\langle \phi \rangle \simeq 1/m$.

As KRSV discuss, a field theory with this kind of potential could be very interesting. The normal one-particle excitations of the true vacuum would be extremely massive, so it may be that the lowest-mass excitations are extended objects—bubbles of false vacuum with some definite size.²³ (There is perhaps some connection with the ideas of Lee and Wick.¹⁷) With the help of the GEP one may be able to explore this possibility further in the future.

C. The Gaussian well and the δ -function potential

Next, we consider a potential well of finite depth, where the potential levels off to a constant value as $\phi \rightarrow \pm \infty$. As noted in Sec. II [see Fig. 3(b)], the so-called effective potential in such cases is simply a constant, $V_{\text{eff}}(\phi_0) = E_0$, and it is interesting to see how the GEP and 1LEP fare in the same circumstances.

A convenient example to study is an inverted-Gaussian potential

$$V(\phi) = -\frac{\kappa}{l} \exp(-\phi^2/l^2). \quad (3.18)$$

Depending on the parameters, this well admits one or more discrete eigenstates with negative energy, and a continuum of positive-energy scattering states. As $l \rightarrow 0$, with κ fixed, the well becomes deeper and narrower, approaching the form $V(\phi) = \kappa\sqrt{\pi}\delta(\phi)$. Although the potential becomes singular, the physics of this limit is smooth: There is just one bound state, with energy $-\frac{1}{2}\pi\kappa^2$, and whose wave function approaches the form $\exp(-\kappa\sqrt{\pi}|\phi|)$.

This example is a good illustration of just how silly the 1LEP can be. The 1LEP,

$$V_{1l}(\phi_0) = V(\phi_0) + \frac{1}{2}[V''(\phi_0)]^{1/2}, \quad (3.19)$$

is undefined in the large- ϕ region, where $V''(\phi_0)$ is negative, and exists only for $|\phi| < l/\sqrt{2}$. Furthermore, in the central region where it does exist, its behavior is quite perverse: For small l , it is the positive $\frac{1}{2}(V'')^{1/2}$ contribution

that dominates, turning the potential well into an apparent barrier. The effect is clearly seen in Fig. 6 which shows the 1LEP (dotted curve) in the cases $l=0.2, l=0.1$, on the same scale. The rapid growth of the “barrier” height as $l \rightarrow 0$ is evident. This behavior of the 1LEP bears no relation at all to the reality of the physical situation. (Of course, the fact that the one-loop “correction term” is much larger than the classical term is a warning not to trust the one-loop result.)

To calculate the GEP in this case it is easier to use the direct integration method of Eq. (2.7), rather than the a, a^\dagger formalism. The result is

$$V_G(\phi_0, \Omega) = \frac{1}{4}\Omega - \frac{\kappa}{l} \left[\frac{\Omega l^2}{1 + \Omega l^2} \right]^{1/2} \exp \left[\frac{-\Omega \phi_0^2}{1 + \Omega l^2} \right], \quad (3.20)$$

with Ω given by

$$\frac{1}{2}\Omega^{1/2}(1 + \Omega l^2)^{3/2} = \kappa \left[1 - \frac{2\Omega \phi_0^2}{1 + \Omega l^2} \right] \exp \left[\frac{-\Omega \phi_0^2}{1 + \Omega l^2} \right]. \quad (3.21)$$

The result is plotted as the dashed line in Fig. 6 and, for these small l values, it has a very shallow bowl shape, indicating a bound state just below the continuum, near the top of the well. This does correspond to reality.

Note that the GEP lies *below* the classical potential at large ϕ , something which is inherently impossible for the 1LEP. However, this is “right” in the sense that the effective extent of the well is much greater than the width of the classical potential. This is obvious from the δ -function limit, where the classical potential has zero width, yet the exact GS wave function has a finite extent, $\simeq 1/(\kappa\sqrt{\pi})$. However, it must be admitted that the GEP grossly exaggerates this spreading-out effect, as it has an extremely long tail, behaving asymptotically like ϕ_0^{-1} . (As $\phi_0 \rightarrow \infty$ in (3.21),

$$\Omega \rightarrow (2\phi_0^2)^{-1} [1 - (e/8)^{1/2}(\kappa\phi_0)^{-1} + O(\phi_0^{-2})],$$

resulting in $\bar{V}_G(\phi_0) \rightarrow -(2e)^{-1/2}\kappa/\phi_0$.)

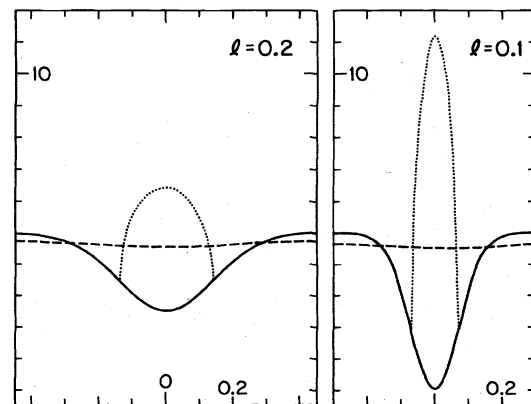


FIG. 6. The Gaussian potential well, Eqs. (3.18) with $\kappa=1$ and $l=0.2, 0.1$, illustrating the approach to the δ -function limit, $l \rightarrow 0$. Dashed curve = GEP; dotted curve = 1LEP.

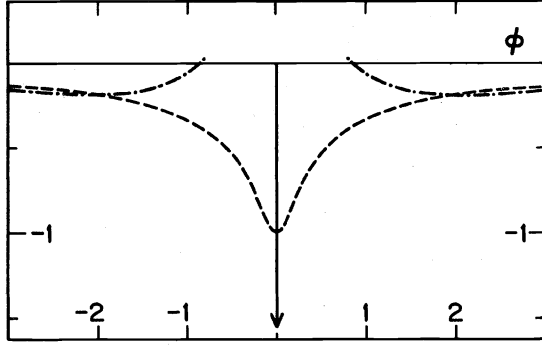


FIG. 7. The δ -function potential $V = -\sqrt{\pi}\delta(\phi)$, with its associated GEP (dashed curve). The dot-dashed curve represents the first-excited-state generalization of the GEP (though see text for explanation).

The shape of the GEP in the δ -function limit is shown in Fig. 7. Note that the value at $\phi_0 = 0$ is $-\kappa^2$, to be compared with the exact eigenvalue $-\frac{1}{2}\pi\kappa^2$.

The next question to consider concerns the excited states. There should be none, when l is small. Does the GEP approach see this, and, if so, how? To answer these questions we compute the excited-state generalizations of the GEP. Again we use the direct integration approach, with the excited oscillator states used as trial wave functions being written out explicitly as Hermite polynomials times a Gaussian. For example, to construct $\bar{V}_{G,1}(\phi_0)$ one uses

$$\psi = (2\Omega)^{1/2} \left(\frac{\Omega}{\pi} \right)^{1/4} (\phi - \phi_0) \exp\left[-\frac{1}{2}\Omega(\phi - \phi_0)^2\right]. \quad (3.22)$$

For simplicity we quote the result only for the δ -function limit, $l \rightarrow 0$ (the behavior for small, finite l is qualitatively similar):

$$V_{G,1}(\phi_0, \Omega) = \frac{3}{4}\Omega - 2\kappa\phi_0^2\Omega^{3/2}\exp(-\Omega\phi_0^2), \quad (3.23)$$

with

$$1/(2\Omega^{1/2}) = 2\kappa\phi_0^2(1 - \frac{2}{3}\Omega\phi_0^2)\exp(-\Omega\phi_0^2). \quad (3.24)$$

The optimization condition for Ω has a very different character from Eq. (3.21) above. At large ϕ_0 there are two solutions: the smaller- Ω solution corresponds to a local maximum of $V_{G,1}(\phi_0, \Omega)$, so it is the larger- Ω solution which is relevant. When inserted into Eq. (3.23), this Ω gives rise to the dot-dashed curve in Fig. 7. As ϕ_0 is decreased, the two solutions come together, coalesce, and then disappear for $\phi_0 < \phi_{0,\text{crit}} = (0.7685)\kappa^{-1}$. In the small- ϕ_0 region there is no solution because $V_{G,1}(\phi_0, \Omega)$ is a monotonic-increasing function of Ω . Its minimum value occurs at the end point $\Omega = 0$, where $V_{G,1} = 0$. (We did not encounter this situation in the earlier examples be-

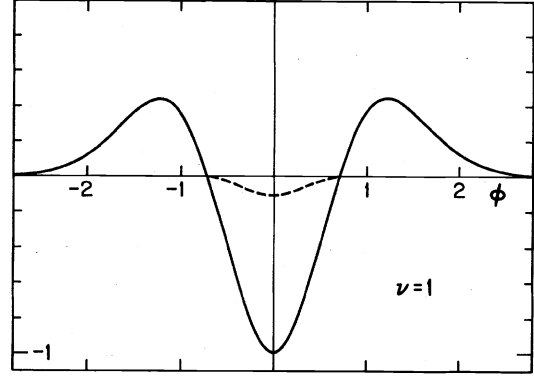


FIG. 8. The "crater potential," Eq. (3.25) with $U=l=1$ and $\nu=1$. Its associated GEP is the dashed curve, shown enlarged in Fig. 9.

cause there $\Omega \rightarrow 0$ gave rise to an "infrared divergence." Here, since the potential is bounded above, an infinitely spread-out wave function has finite energy.) Note that the end point $\Omega = 0$ actually takes over from Eq. (3.24) as soon as the latter starts to give a value for $V_{G,1}$ which is greater than the end-point value of zero. This breakpoint occurs at $|\phi_0| = \phi_{0,\text{break}} = (0.8744)\kappa^{-1}$, just before the solution to (3.24) disappears. Thus, $\bar{V}_{G,1}(\phi_0)$ is given by the dot-dashed curve for $|\phi_0| > \phi_{0,\text{break}}$, where it crosses the axis, and equals zero for $|\phi_0| \leq \phi_{0,\text{break}}$.

The large- ϕ_0 behavior of $\bar{V}_{G,1}(\phi_0)$ seems peculiar, especially as it lies *below* the GEP itself. This must be admitted to be an artificial pathology, unrelated to any real physics. However, from the behavior at small ϕ_0 , one would naturally conclude that the potential does not admit any excited states—which is indeed the case.

D. The crater potential

An interesting variant of the potential studied in the previous subsection is the form

$$V(\phi) = U(-1 + 2\nu\phi^2/l^2)\exp(-\phi^2/l^2), \quad (3.25)$$

in which the central well is guarded on each side by "crater walls" (see Fig. 8). In the previous case of a rimless bowl-shaped potential, there was always at least one bound state. Here, it is possible for there to be none. This happens if ν is too large, when the narrowness of the central well pushes the energy of the would-be ground state above zero. It then becomes metastable; a resonance which can decay into the continuum of unbound, non-normalizable, scattering states. We can see this effect nicely through the GEP, and the results are instructive because they bear a striking similarity to the behavior found in ϕ^4 field theory in $3+1$ dimensions.⁸

Calculating $V_G(\phi_0, \Omega)$ we find

$$V_G(\phi_0, \Omega) = \frac{1}{4l^2} \frac{x}{(1-x)} - Ux^{1/2}[(1-\nu) + \nu x(1-2x\phi_0^2/l^2)]\exp(-x\phi_0^2/l^2), \quad (3.26)$$

where

$$x \equiv \Omega l^2 / (1 + \Omega l^2). \quad (3.27)$$

As usual, this expression has to be minimized with respect to Ω , for $0 < \Omega < \infty$. The stationarity condition $dV_G/d\Omega = 0$ gives the equation

$$U \exp(-x\phi_0^2/l^2) [(1-\nu)(1-2x\phi_0^2/l^2) + \nu x(3-12x\phi_0^2/l^2 + 4x^2\phi_0^4/l^4)] - x^{1/2}/[2l^2(1-x)^2] = 0. \quad (3.28)$$

However, in this example it can be that the global minimum of V_G occurs at the end point $\Omega=0$, where $V_G(\phi_0, \Omega)=0$.

For illustrative purposes we set $U=l=1$ and consider the two cases $\nu=1$ and $\nu=1.5$. For $\nu=1$ the potential is shown in Fig. 8, with $\bar{V}_G(\phi_0)$ superimposed. The GEP is shown on a larger scale in Fig. 9. What happens is this. The stationarity condition, Eq. (3.28) has two solutions for Ω at small ϕ_0 . The relevant solution has the larger Ω value: the other solution corresponds to a local *maximum* of $V_G(\phi_0, \Omega)$. The two solutions coalesce and then disappear when ϕ_0 exceeds $\phi_{0,\text{crit}}=0.9114$. Thereafter, Eq. (3.28) has no solution. However, before this happens, the local minimum found from (3.28) ceases to be the *global* minimum, and at $\phi_0=\phi_{0,\text{break}}=0.7587$ the end point $\Omega=0$ takes over. Thus, for $\phi_0 > \phi_{0,\text{break}}$ one has $\bar{V}_G(\phi_0)=0$. (See Fig. 9.) Exactly the same behavior is seen in the GEP for $(\phi^4)_{3+1}$ field theory.^{6,8}

In the present case, the physical interpretation is clear: There is a ground state, centered on $\phi_0=0$, of roughly the usual harmonic-oscillator type, with a continuum of energy levels above it, corresponding to nonlocalized "ionized" states. (The obvious field-theory analogy would be an ordinary field theory at low temperatures, with a phase transition to more exotic behavior at high temperatures.)

For larger values of ν , as we said, the would-be ground state in the well is pushed to higher energies and becomes an unstable resonance. We see this in the case $\nu=1.5$, shown in Fig. 10. Here, $\Omega=0$ is always the global minimum of $V_G(\phi_0, \Omega)$, and so $\bar{V}_G(\phi_0)$ coincides with the ϕ_0 axis everywhere. However, the local maximum and local minimum solutions of (3.28), still existing at small ϕ_0 , give rise to the "ghostly grin" in Fig. 10. The lower of these two dotted curves can be interpreted as the "potential well" in which the resonance sits, and its minimum provides an estimate of the resonance energy.

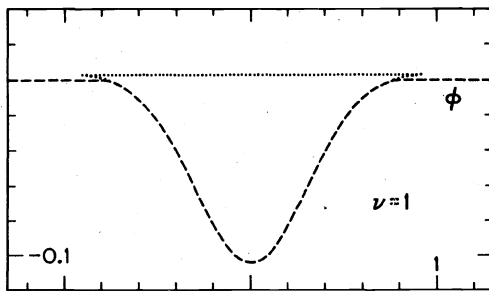


FIG. 9. A close-up of the GEP for the crater potential of Fig. 8. The dashed line, including the horizontal sections extending to $\pm\infty$, is the GEP. The dotted lines indicate the inoperative local-minimum and local-maximum solutions of the optimization equation (3.28).

According to the GEP, the "phase transition" between the two behaviors (existence or nonexistence of a unique, normalizable ground state) occurs at $\nu=1.3067$. The true critical value of ν is presumably slightly larger than this, since the GEP is giving us only an upper bound on the GS energy. [Again, there is a direct analogy with the $(\phi^4)_{3+1}$ results, which show a similar phase transition between weak and strong coupling regimes.^{6,8}]

IV. COUPLED FIELDS

A. The O(2)-symmetric AHO and the Goldstone potential

We now turn to the case of two coupled fields in $0+1$ dimensions—or, in QM language, a two-dimensional system:

$$H = \frac{1}{2}p_1^2 + \frac{1}{2}p_2^2 + V(\phi_1, \phi_2). \quad (4.1)$$

Our trial wave function will now be a two-dimensional Gaussian, $\exp(-\frac{1}{2}\phi_i\Omega_{ij}\phi_j)$, where the frequency parameter Ω now becomes a symmetric matrix, Ω_{ij} . Thus, the ansatz involves three variational parameters; two principal frequencies Ω_1, Ω_2 , and an angle θ specifying the orientation of the principal axes of the wave function with respect to the ϕ_1, ϕ_2 axes. In terms of the a, a^\dagger formalism, we need to generalize Eq. (2.8) to

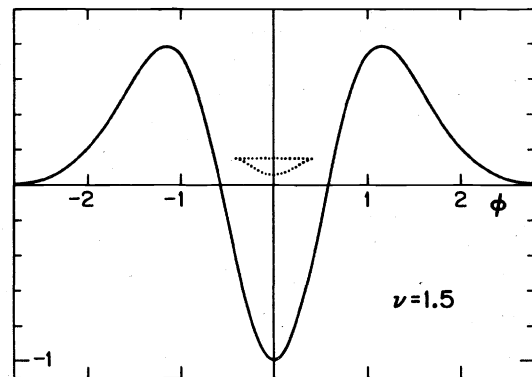


FIG. 10. The "crater potential," Eq. (3.25) with $U=l=1$ and $\nu=1.5$. The GEP coincides with the ϕ axis. However, the inoperative local-minimum solution for $\bar{\Omega}$ (shown, together with the local-maximum solution, as the dotted curves) can be interpreted as indicating a metastable, resonant state in the central well.

$$\begin{bmatrix} \phi_1 \\ \phi_2 \end{bmatrix} = \begin{bmatrix} \phi_{0,1} \\ \phi_{0,2} \end{bmatrix} + \begin{bmatrix} \cos\theta & -\sin\theta \\ \sin\theta & \cos\theta \end{bmatrix} \begin{bmatrix} (2\Omega_1)^{-1/2}(a_1 + a_1^\dagger) \\ (2\Omega_2)^{-1/2}(a_2 + a_2^\dagger) \end{bmatrix}, \quad (4.2)$$

$$\begin{bmatrix} p_1 \\ p_2 \end{bmatrix} = \begin{bmatrix} \cos\theta & -\sin\theta \\ \sin\theta & \cos\theta \end{bmatrix} \begin{bmatrix} -\frac{1}{2}i(2\Omega_1)^{1/2}(a_1 - a_1^\dagger) \\ -\frac{1}{2}i(2\Omega_2)^{1/2}(a_2 - a_2^\dagger) \end{bmatrix}.$$

The generalization to many fields should be obvious.

We apply this formalism first to the O(2)-symmetric AHO potential

$$V(\vec{\phi}) = \frac{1}{2}m^2\vec{\phi}^2 + \lambda(\vec{\phi}^2)^2, \quad (4.3)$$

where $\vec{\phi}^2 \equiv \phi_1^2 + \phi_2^2$. The necessary matrix elements are easily evaluated:

$$\begin{aligned} \langle 0 | \frac{1}{2}p_1^2 + \frac{1}{2}p_2^2 | 0 \rangle &= \frac{1}{4}(\Omega_1 + \Omega_2), \\ \langle 0 | \vec{\phi}^2 | 0 \rangle &= \vec{\phi}_0^2 + (2\Omega_1)^{-1} + (2\Omega_2)^{-1}, \\ \langle 0 | (\vec{\phi}^2)^2 | 0 \rangle &= (\vec{\phi}_0^2)^2 + 3(2\Omega_1)^{-2} + 3(2\Omega_2)^{-2} + 2(2\Omega_1)^{-1}(2\Omega_2)^{-1} + 2\vec{\phi}_0^2[(2\Omega_1)^{-1} + (2\Omega_2)^{-1}] \\ &\quad + 4(2\Omega_1)^{-1}(\phi_{0,1}\cos\theta + \phi_{0,2}\sin\theta)^2 + 4(2\Omega_2)^{-1}(-\phi_{0,1}\sin\theta + \phi_{0,2}\cos\theta)^2. \end{aligned} \quad (4.4)$$

From this it is clear that the minimization of V_G with respect to θ will require

$$\tan\theta = \phi_{0,2}/\phi_{0,1} \text{ or } -\phi_{0,1}/\phi_{0,2}. \quad (4.5)$$

The two choices are equivalent, and correspond to the principal axes of the Gaussian wave function being aligned radially and transversely. Changing notation slightly, we denote the radial and transverse frequencies by Ω and ω , respectively. We can then write \bar{V}_G as

$$\begin{aligned} \bar{V}_G(\vec{\phi}_0) &= \frac{1}{4}(\Omega + \omega) + \frac{1}{2}m^2[\vec{\phi}_0^2 + (2\Omega)^{-1} + (2\omega)^{-1}] \\ &\quad + \lambda[(\vec{\phi}_0^2)^2 + 3(2\Omega)^{-2} + 3(2\omega)^{-2} + 2(2\Omega)^{-1}(2\omega)^{-1} + 6\vec{\phi}_0^2(2\Omega)^{-1} + 2\vec{\phi}_0^2(2\omega)^{-1}] \end{aligned} \quad (4.6)$$

with Ω and ω being given by

$$\begin{aligned} -\frac{1}{4}\Omega + \frac{1}{4}\frac{m^2}{\Omega} + \lambda\left[\frac{3}{2\Omega^2} + \frac{1}{2\Omega\omega} + \frac{3\vec{\phi}_0^2}{\Omega}\right] &= 0, \\ -\frac{1}{4}\omega + \frac{1}{4}\frac{m^2}{\omega} + \lambda\left[\frac{3}{2\omega^2} + \frac{1}{2\Omega\omega} + \frac{\vec{\phi}_0^2}{\omega}\right] &= 0. \end{aligned} \quad (4.7)$$

Note that one will have $\omega = \Omega$ at $\vec{\phi}_0^2 = 0$, but not elsewhere. As before, we can use these conditions to simplify the expression for \bar{V}_G , yielding

$$\bar{V}_G(\vec{\phi}_0) = V(\vec{\phi}_0) + \frac{1}{2}(\Omega + \omega) - \frac{\lambda}{4\Omega^2\omega^2}(3\Omega^2 + 3\omega^2 + 2\Omega\omega). \quad (4.8)$$

It is particularly interesting to look at the $m^2 < 0$ case, where the potential has a "Mexican hat" shape. [In QFT terms, this is the (0+1)-dimensional version of the Goldstone model.] Results for the cases $\xi^2 \equiv m^2/(2\lambda)^{2/3}$, $= -1$ and -10 are shown in Fig. 11, the graphs showing a radial slice through the potential. By comparison with the equivalent results for the ordinary AHO (Fig. 4), we see that the quantum effects are more pronounced in the O(2) case. Again we see "symmetry restoration" by quantum effects in the $\xi^2 = -1$ case, while the ground state remains at nonzero ϕ_0 for $\xi^2 = -10$. In the latter case we note that at the minimum, $|\vec{\phi}_0| = 3.64$, the values of Ω and ω are 1.29 and 0.36, respectively. Thus, the wave function is much more spread out in the transverse than in the radial direction, exactly as one would expect. Note,

however, that ω is not zero; the curvature of the outer wall of the potential limits the transverse spread of the Gaussian wave function. Related to this is the fact that if we compute the energy of the first transverse excitation, it lies a finite amount above the ground state. There is no Goldstone theorem in 0+1 dimensions.²⁴ The ubiquitous $(2\omega)^{-1}$ factors represent severe infrared divergences which prevent the appearance of a zero-frequency mode. [The situation is similar in 1+1 dimensions, where Coleman's theorem²⁵ forbids the appearance of massless bosons. In higher dimensions the analogs of the $(2\omega)^{-1}$ factors are no longer infrared divergent, and massless bosons may arise.]

We can obtain the 1LEP as before by dropping order- \hbar^2 terms in Eq. (4.6), together with the terms they produce in Eqs. (4.7). Although in this section we have been setting

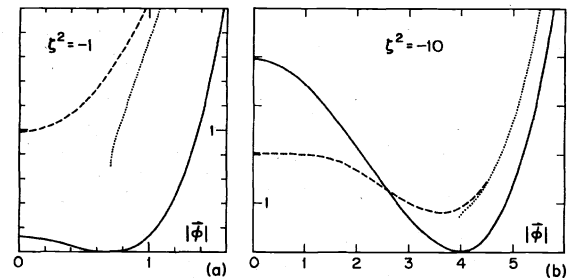


FIG. 11. A radial slice through the Goldstone potential; Eq. (4.3) with $m^2 < 0$. Conventions as in Fig. 4.

$\hbar=1$, it is easy to see, by referring back to Sec. II, that the \hbar^2 terms are those with denominator $(2\Omega)^2$, $(2\omega)^2$ or $(2\Omega)(2\omega)$. This leads to

$$V_{1l}(\vec{\phi}_0) = V(\vec{\phi}_0) + \frac{1}{2}(\Omega + \omega), \quad (4.9)$$

with

$$\begin{aligned} \Omega &= (m^2 + 12\lambda\vec{\phi}_0^2)^{1/2}, \\ \omega &= (m^2 + 4\lambda\vec{\phi}_0^2)^{1/2}, \end{aligned} \quad (4.10)$$

which are the square roots of the second derivatives of $V(\vec{\phi}_0)$ in the radial and transverse directions, respectively. Thus, the 1LEP becomes undefined for $\vec{\phi}_0^2 < |m^2|/(4\lambda)$, i.e., inside the circle of classical vacua, and has the strange appearance shown in the dotted curves of Fig. 11.

B. A coupled oscillator model with dynamical mass generation

Our final example is the potential

$$V(\phi, \chi) = \frac{1}{2}m^2\phi^2 + g\phi^2\chi^2, \quad (4.11)$$

which, in QFT terms, describes a massive field ϕ coupled to a massless field χ . As we shall see, the interaction dynamically generates a mass for the χ field.²⁶ In QM language, the system consists of a particle in a long, flat valley running along the χ axis. A contour map of this valley is shown in Fig. 12 for $m^2=g=1$. For $\chi=0$ the valley is relatively broad, with the sides rising like $\frac{1}{2}m^2\phi^2$, but to either side the valley becomes narrower, with the walls rising like $(\frac{1}{2}m^2 + g\chi^2)\phi^2$.

Classically, the vacuum is degenerate: the particle is equally happy to sit anywhere on the χ axis ($\phi=0$, χ arbitrary). However, the quantum claustrophobia of the particle causes it to shun the narrow ends of the potential, and favor the broad part of the valley near the origin. Classically, the particle could escape to infinity, but, ironically, the restlessness induced by QM fluctuations ensures that it remains trapped.

Again, it is natural to describe this phenomenon in terms of an effective potential. Going away from the ori-

gin along the χ axis, the particle feels an increasing zero-point energy associated with its transverse fluctuations in the narrowing valley. This makes the effective potential seem to curve upward, even in the χ direction, causing an effective restoring force back toward the origin. In QFT terms, the induced curvature, being an "effective" χ^2 term, is a dynamically generated mass.

This is exactly the kind of intuition that the GEP embodies. To calculate \bar{V}_G we proceed as in Sec. IV A, though we quickly find that the appropriate angle θ is always zero. This means that the frequency parameters Ω and ω can be identified as associated with the ϕ and χ fields, respectively. The result can be written as

$$\bar{V}_G(\phi_0, \chi_0) = V(\phi_0, \chi_0) + \frac{1}{2}(\Omega + \omega) - g/(4\Omega\omega), \quad (4.12)$$

with

$$\begin{aligned} \Omega^2 &= m^2 + g(2\chi_0^2 + 1/\omega), \\ \omega^2 &= g(2\phi_0^2 + 1/\Omega). \end{aligned} \quad (4.13)$$

We illustrate the results for the case $m^2=g=1$ in Fig. 13 as a contour map of \bar{V}_G . This shows the effective potential rising in all directions outward from the origin, just as we expected. The crucial point is that ω , the frequency parameter associated with the χ field, is nonzero.

[There is a subtle point concerning the precise definition of the "dynamically generated mass" here. We think it is best defined as the physically observable quantity $E_1 - E_0$, the energy gap between the ground state and the first excited state. In field theory, a one-quantum state has energy $(\vec{k}^2 + m_{\text{phys}}^2)^{1/2} + E_0$, and so the smallest-energy excitation is indeed m_{phys} . In field theory this definition coincides with the curvature of the effective potential at the origin, but this equivalence is not true in QM. We think it best to stick to the physically based definition, rather than the formal one. For $m^2=g=1$ we find $m_{\text{dyn}} \equiv E_1 - E_0 = 0.284$, which is very different from

$$\partial^2 \bar{V}_G / \partial \chi_0^2 |_{\phi_0=\chi_0=0} = \omega |_{\phi_0=\chi_0=0} = 0.819.]$$

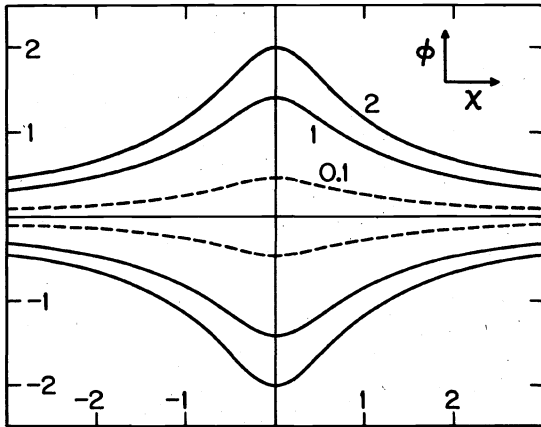


FIG. 12. Equipotentials of $V = \frac{1}{2}m^2\phi^2 + g\phi^2\chi^2$, with $m^2=g=1$, for energies $E=0.1, 1, 2$.

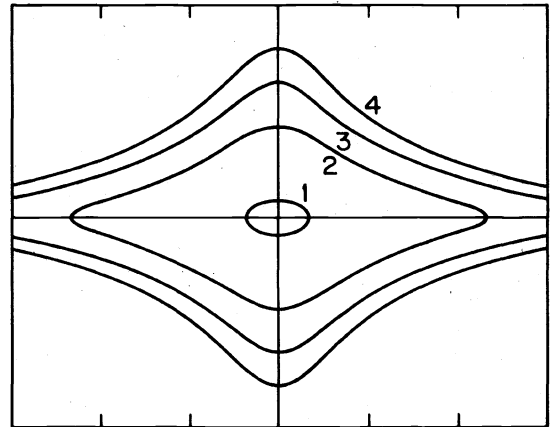


FIG. 13. Contours of the GEP corresponding to the potential of Fig. 12, for energies $E=1, 2, 3, 4$. The value of the GEP at the origin is $E_0^{(G)} = 0.950$.

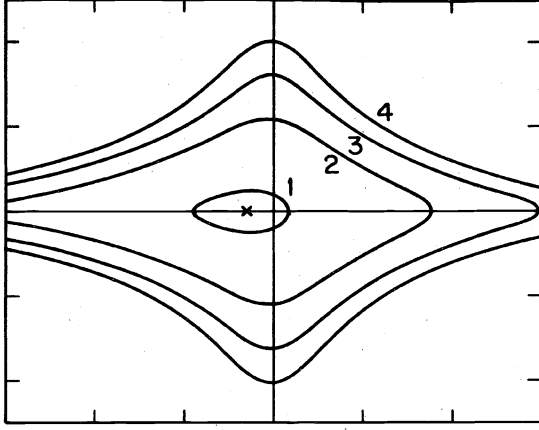


FIG. 14. As Fig. 13, showing the effect on the GEP of an extra $\eta\chi$ term in the potential, for $\eta=0.2$. The contours remain closed curves. The minimum is displaced to $\chi_0 = -0.313$, and the energy is lowered to $E_0^{(G)} = 0.919$.

Our example can be made more dramatic by adding a linear term $+\eta\chi$ to the potential. Then the valley slopes steadily downward to the left. Classically, the potential is unbounded below, so the system has no ground state: the particle accelerates off toward $\phi=0, \chi=-\infty$. However, provided that the slope given to the valley floor is sufficiently gentle, the quantum-claustrophobia effect will continue to dominate and the particle will remain localized somewhere just to the left of the origin. This is illustrated in Fig. 14 for $m^2=g=1$ with $\eta=0.2$. According to the GEP, a ground state exists provided $|\eta| < (\frac{1}{2}g)^{1/2}$, so for small η we have another example of “quantum-mechanical resuscitation.” (Note that in this example the QM effects could not overcome a negative-mass-squared term. One would need, say, a $\chi^2\phi^4$ coupling to accomplish this. See, e.g., Ref. 27.)

The special case $m^2=0$, i.e., $V(\phi, \chi) = g\phi^2\chi^2$, where both fields are classically massless, is particularly interest-

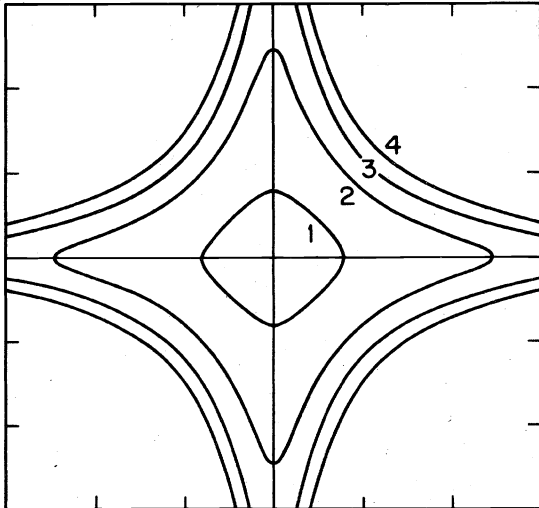


FIG. 15. Contours of the GEP corresponding to $V = g\phi^2\chi^2$. The value at the origin is $E_0^{(G)} = \frac{3}{4}g^{1/3}$.

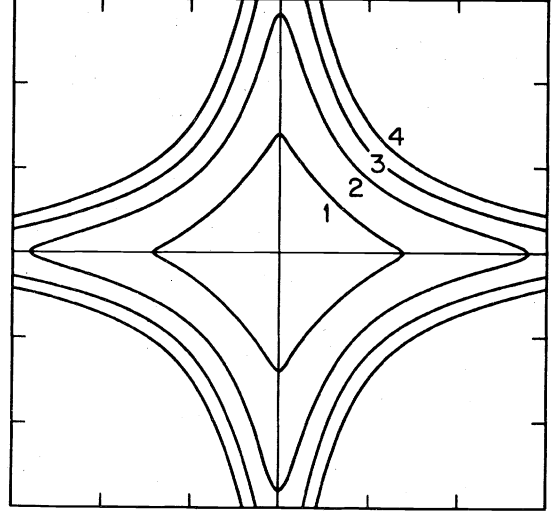


FIG. 16. Contours of the 1LEP for $V = g\phi^2\chi^2$. The equipotentials have right-angle corners where they cross the axes. The value at the origin is zero.

ing. It has been studied recently by Simon,²⁸ who gives several rigorous proofs that a unique ground state exists. The first of these proofs is directly related to the intuitive ideas we have been using here. A contour plot of the GEP is shown in Fig. 15. The GEP's estimate of the GS energy is $0.75g^{1/3}$, which compares well with the numerical result²⁹ $0.698g^{1/3}$. The dynamically generated mass $m_{\text{dyn}} \equiv E_1 - E_0 = 0.344g^{1/3}$.

To be fair to the 1LEP, we should say that it is also able to see the dynamical mass generation. However, it does have the slight pathology that it is not differentiable on the χ axis (nor on the ϕ axis if $m^2=0$). For the $m^2=0$ case the 1LEP has the form

$$V_{1l} = g\phi_0^2\chi_0^2 + (\frac{1}{2}g)^{1/2}(|\phi_0| + |\chi_0|), \quad (4.14)$$

whose contours have right-angle corners where they intersect the axes. See Fig. 16. Note that the implied estimate of the GS energy is zero, which compares poorly with the exact result $0.698g^{1/3}$ quoted above.

V. DISCUSSION AND CONCLUSIONS

Our motivation in defining the GEP²⁻⁷ was to obtain a general picture of the basic physics of a given system; a picture embodying our intuitive ideas of what quantum fluctuations do. From the QM examples studied here it seems that the GEP performs this role rather well. Of course, in QM—where, from a glance at the potential, one can more or less guess the basic physics—the concept has little practical use. However, in field theory, where our intuition is much less well developed, the GEP gives us a potentially valuable means of “calculating our intuition.”

Three major questions remain to be considered. The first is the generalization to field theory, which we shall discuss in the second paper of this series (see also Refs. 2–6, of course). The second question is how to judge the reliability of the GEP results: under what circumstances

will the approximation do poorly, and how can one estimate the error? The third question is what to do next: having calculated the GEP for some problem, how does one set about improving the results? These last two questions need further attention, but we offer here a few preliminary observations.

As the GEP approach is based on harmonic-oscillator wave functions, one might think that it can only work in situations where the classical potential is approximately parabolic near its minimum. This naive supposition is too pessimistic. The GEP continues to work excellently for a pure- ϕ^4 potential, and is satisfactory even in such extreme cases as a δ -function potential, and the hydrogen atom problem (see later). It seems more pertinent to require that the GEP itself, rather than the classical potential, should be approximately parabolic close to its minimum. Let the minimum of the GEP be $\bar{V}_G(\phi_{0,\min}) = E_0^{(G)}$, and let Ω_{\min} be the associated value of the Ω parameter. Then, since the trial GS wave function has a width $\simeq \Omega_{\min}^{-1/2}$, the GEP picture is self-consistent only if $\bar{V}_G(\phi_0)$ looks roughly like $E_0^{(G)} + \frac{1}{2}\Omega_{\min}^2(\phi_0 - \phi_{0,\min})^2$ in the region $\phi_{0,\min} \pm \Omega_{\min}^{-1/2}$. The more this condition is violated, the worse one should expect the error to be. Looking back at our examples, this idea does seem to have

some validity. However, we have been unable to devise an approach to error estimation that carries over naturally to field theory. This is an important problem.

On the third question, of how to systematically improve the results, we have some more concrete ideas. The essential point, as hinted earlier, is to regard the GEP result as the first order in a perturbation series, in analogy to the CK method.¹⁰⁻¹² The only new feature is to incorporate a possible shift of the field: $\phi \rightarrow \phi_0 + \hat{\phi}$. If the Hamiltonian is

$$H = \frac{1}{2}p^2 + V(\phi), \quad (5.1)$$

we propose to write it in the form

$$H = H_0 + H_{\text{int}}, \quad (5.2)$$

with³⁰

$$H_0 = V(\phi_0) + \frac{1}{2}(p^2 + \Omega^2 \hat{\phi}^2), \quad (5.3)$$

$$H_{\text{int}} = V(\phi_0 + \hat{\phi}) - V(\phi_0) - \frac{1}{2}\Omega^2 \hat{\phi}^2,$$

and follow the usual Rayleigh-Schrödinger perturbation procedure. For example, the j th eigenvalue would be calculated as

$$E_j = E_j^{(0)} + \Omega \langle j | H_{\text{int}} | j \rangle_{\Omega} + \sum_{n \neq j} \frac{\Omega \langle j | H_{\text{int}} | n \rangle_{\Omega} \Omega \langle n | H_{\text{int}} | j \rangle_{\Omega}}{E_j^{(0)} - E_n^{(0)}} + \dots, \quad (5.4)$$

where $E_j^{(0)} = V(\phi_0) + (j + \frac{1}{2})\Omega$. At each order the result will depend on the arbitrary parameter Ω , which we propose to fix by the "principle of minimal sensitivity"²⁰ as in the CK method.^{10,11} That is, at each order, we require our approximant to be stationary with respect to Ω ; the point being that the exact result is Ω independent, so the approximation can only be good where it is approximately Ω independent. (See Ref. 20 for further discussion of this point and subtleties with multiple stationary points, etc.) It is most important that Ω is *not* fixed "once and for all," but is adjusted separately for each physical quantity, and for each order of approximation. This flexibility is vital to the success of the procedure in low orders, and to its convergence in higher orders.^{10,11,20} Similar remarks also apply to the ϕ_0 parameter.

In first order this procedure gives

$$E_j^{(1)} = \min_{\phi_0, \Omega} (E_j^{(0)} + \Omega \langle j | H_{\text{int}} | j \rangle_{\Omega})$$

$$= \min_{\phi_0, \Omega} \langle j | H | j \rangle_{\Omega}, \quad (5.5)$$

which reproduces the GEP result. [Keeping the dependence on ϕ_0 would give $\bar{V}_{G,j}(\phi_0)$.] Higher orders are straightforward, if tedious. For the AHO this is the CK procedure: for the DWP there is a difference in that the optimum shift parameter ϕ_0 is not necessarily zero. The generalization to field theory is again straightforward (though at some stage it will probably become advisable to devise a manifestly covariant formalism, i.e., to reinvent

Feynman diagrams).

The beauty of this approach is the "benevolent paradox" that one can obtain good, nonperturbative results from a familiar technique—perturbation theory. In field theory we are constrained by the fact that we can basically only do Gaussian functional integrations. Our point is that this does not doom us to conventional perturbation theory and weak-coupling or semiclassical methods. With a little more flexibility, we can obtain vastly better results from calculations of comparable difficulty. The results do not have to be forced into the straitjacket of an expansion in powers of \hbar , or in powers of a coupling constant.

Of course, our examples, together with the work of CK,¹⁰⁻¹² only show that the method works in QM: How well it performs in field theory is a matter for conjecture. However, the GEP approach should be viewed in comparison to the usual perturbation-theory/loop-expansion methods, and *it can only be better*. From the discussion in Sec. II and from the examples, it seems clear that the 1LEP is merely a "cheap" version of the GEP. It works only when it approximates the GEP closely: when it differs it is generally a disaster.

For our parting shot, we return to the hydrogen atom problem $V(r) = -1/r$, with $r^2 = \phi_1^2 + \phi_2^2 + \phi_3^2$. The GEP analysis is rather messy, but qualitatively it is easy to see that $\bar{V}_G(\phi_0)$ resembles the dashed line in Fig. 1. It is also easy to calculate the GEP's estimate of the GS energy, which is $-4/(3\pi\hbar^2) = -0.424\hbar^{-2}$, compared to the exact result of $-0.5\hbar^{-2}$. Contrast this success with the 1LEP which is everywhere complex, and whose real part (which is just the classical potential) remains unbounded below.

Suppose we had only the loop-expansion technique: Would we ever have understood atomic physics?

ACKNOWLEDGMENTS

It is a pleasure to thank Dr. J. Killingbeck of the University of Hull for hospitality and for sharing his vast knowledge of quantum mechanics. I also benefited from

many enjoyable discussions with Graham Shore, especially in relation to the work of Ref. 23. Thanks also to Charles Goebel and Francis Halzen for comments on the original manuscript. This research was supported in part by the University of Wisconsin Research Committee with funds granted by the Wisconsin Alumni Research Foundation, and in part by the Department of Energy under Contract No. DE-AC02-76ER00881.

- ¹S. Coleman and E. Weinberg, *Phys. Rev. D* **7**, 1888 (1973); S. Weinberg, *ibid.* **7**, 2887 (1973); R. Jackiw, *ibid.* **9**, 1686 (1974).
- ²T. Barnes and G. I. Ghandour, *Phys. Rev. D* **22**, 924 (1980).
- ³J. Kuti (unpublished), as discussed in J. M. Cornwall, R. Jackiw, and E. Tomboulis, *Phys. Rev. D* **10**, 2428 (1974).
- ⁴S. J. Chang, *Phys. Rev. D* **12**, 1071 (1975); **13**, 2778 (1976); *Phys. Rep.* **23C**, 301 (1975); S. J. Chang and J. A. Wright, *Phys. Rev. D* **12**, 1595 (1975).
- ⁵M. Weinstein, S. Drell, and S. Yankielowicz, *Phys. Rev. D* **14**, 487 (1976); K. Huang and D. R. Stump, *ibid.* **14**, 223 (1976).
- ⁶W. A. Bardeen and M. Moshe, *Phys. Rev. D* **28**, 1372 (1983); W. A. Bardeen, M. Moshe, and M. Bander, *Phys. Rev. Lett.* **52**, 1188 (1984).
- ⁷The approach here was most heavily influenced by the work of Barnes and Ghandour (Ref. 2), which in turn has its origins in early variational studies of field theory in the 1960's [L. I. Schiff, *Phys. Rev.* **130**, 458 (1963); G. Rosen, *ibid.* **173**, 1632 (1968), and references therein]. The Schrödinger representation and variational methods in field theory were considered by Kuti, whose work is discussed in the interesting article of Cornwall, Jackiw, and Tomboulis (Ref. 3). Unfortunately, we have been unable to locate a published account of this work. A generalized Hartree method was studied extensively by Chang (Ref. 4), in particular for ϕ^4 theory in $1+1$ dimensions. The Hartree method applied to the ground state is entirely equivalent to the Gaussian variational approach, as noted in Ref. 3. (For the excited states there is a difference, and the Hartree procedure is somewhat less successful in estimating the higher eigenvalues of the AHO.) Other variational calculations, motivated by bag-model ideas, can be found in Ref. 5. In Ref. 6 the variational approach is used together with the $1/N$ expansion to study $O(N)$ -symmetric ϕ^4 theory in four dimensions and ϕ^6 theory in three dimensions.
- ⁸P. M. Stevenson, UW-Madison report (unpublished). A brief account of the results for $(\phi^4)_{3+1}$ theory is given in MAD/TH/139, 1983 (unpublished) (*Z. Phys.* to be published).
- ⁹C. M. Bender and T. T. Wu, *Phys. Rev.* **184**, 1231 (1969), Appendix A.
- ¹⁰W. E. Caswell, *Ann. Phys. (N.Y.)* **123**, 153 (1979).
- ¹¹J. Killingbeck, *J. Phys. A* **14**, 1005 (1981); E. J. Austin and J. Killingbeck, *ibid.* **15**, L443 (1982); J. Killingbeck, *Microcomputer Quantum Mechanics* (Adam Hilger, Bristol, England, 1983).
- ¹²I. G. Halliday and P. Suranyi, *Phys. Lett.* **85B**, 421 (1979); *Phys. Rev. D* **21**, 1529 (1980). This approach is somewhat different from the CK method, being based on a *squared* harmonic-oscillator Hamiltonian as H_0 . To first order, however, it is equivalent. In QM the Halliday-Suranyi approach is definitely superior, but it seems very hard to extend it to field theory. For a gallant attempt, see J. M. Rabin, *Nucl. Phys. B* **224**, 308 (1983).
- ¹³S. Dimopoulos and H. Georgi, *Phys. Lett.* **117B**, 287 (1982).
- ¹⁴Strictly speaking, this is inaccurate, because in QM, unlike QFT, the symmetry is never actually broken. Even for a potential which retains a double-well character, the true ground state is a symmetric superposition of the GS wave functions in the two wells, and has $\langle\phi\rangle=0$. In fancy language, the symmetry is always restored by instanton effects.
- ¹⁵J. Goldstone, A. Salam, and S. Weinberg, *Phys. Rev.* **127**, 965 (1962); G. Jona-Lasinio, *Nuovo Cimento* **34**, 1790 (1964); see also Ref. 1, and E. S. Abers and B. W. Lee, *Phys. Rep.* **9C**, 1 (1973); pp. 91–99.
- ¹⁶T. L. Curtright and C. B. Thorn, *J. Math. Phys.* **25**, 541 (1984).
- ¹⁷K. Symanzik, *Commun. Math. Phys.* **16**, 48 (1970); T. D. Lee and G. C. Wick, *Phys. Rev. D* **9**, 2291 (1974).
- ¹⁸D. J. E. Callaway and D. J. Maloof, *Phys. Rev. D* **27**, 406 (1983); D. J. E. Callaway, *ibid.* **27**, 2974 (1983); R. J. Rivers, *Z. Phys.* **22**, 137 (1984).
- ¹⁹We do not use this name because Ω at $\phi_0=0$ is not the energy gap between the ground state and the first excited state. While in field theory the mass gap is usually equal to Ω at $\phi_0=0$ (within the GEP approximation), it seems to us that there is still a conceptual distinction.
- ²⁰P. M. Stevenson, *Phys. Rev. D* **23**, 2916 (1981), Sec. II; in *Radiative Corrections in $SU(2)_L \times U(1)$* , proceedings of the Topical Conference edited by B. W. Lynn and J. F. Wheeler (World Scientific, Singapore, 1984).
- ²¹S. K. Kauffmann and S. M. Perez, *J. Phys. A* **17**, 2027 (1984).
- ²²R. Balsa, M. Plo, J. G. Esteve, and A. F. Pacheco, *Phys. Rev. D* **28**, 1945 (1983).
- ²³F. Karsch, E. Rabinovici, G. Shore, and G. Veneziano, *Nucl. Phys. B* **242**, 503 (1984).
- ²⁴It is clear that the proofs in Ref. 15 [see also J. Bernstein, *Rev. Mod. Phys.* **46**, 7 (1974)] collapse in $0+1$ dimensions: with just time and no space, there is no Lorentz symmetry.
- ²⁵S. Coleman, *Commun. Math. Phys.* **31**, 259 (1973).
- ²⁶This example was motivated by the description of how a pseudo-Goldstone boson acquires a mass given by G. Bandelloni, C. Becchi, A. Blasi, and R. Collina, *Commun. Math. Phys.* **67**, 147 (1979). The original references include S. Weinberg, *Phys. Rev. Lett.* **29**, 1698 (1972); *Phys. Rev. D* **7**, 2887 (1973).
- ²⁷J. Makarewicz, *J. Phys. A* **16**, L553 (1983).
- ²⁸B. Simon, *Ann. Phys. (N.Y.)* **146**, 209 (1983), and references therein.
- ²⁹F. T. Hioe, D. MacMillen, and E. W. Montroll, *Phys. Rep.* **43C**, 305 (1978). This number comes from the $c=-1$ entry of Table 9, using the rotation-of-coordinates trick to relate a $(x_1^4 - 2x_1^2x_2^2 + x_2^4)$ potential to a $4\phi^2\chi^2$ potential.
- ³⁰Placing $V(\phi_0)$ in H_0 is just a convenience. Being diagonal in the harmonic-oscillator basis, it does not affect second- or higher-order corrections, which involve only nondiagonal matrix elements.